Laser Induced Fluorescence in high enthalpy facilities in the Tsniimach Center (Moscow – Russia)

L. Robin
CORIA / CNRS UMR 6614
Université de Rouen
Place Emile Blondel
76821 Mont Saint Aignan Cedex
France

SUMMARY

The requirements for accurate measurements, the higher sophistication in the design, the need for monitoring, control and diagnostics in difficult circumstances and the request for data bases to validate numerical codes have incited the advanced measurement techniques to the investigation of ground test facilities.

This lecture presents an experimental work and the results obtained by Laser Induced Fluorescence (LIF) in continuous high enthalpy supersonic airflows. The test campaign is performed at the Central Research Institute of Machine Building (Tsniimach, Moscow region) in ground experimental facilities designed for aerodynamics and heat transfer studies of supersonic and hypersonic aircrafts. The main objective of this test campaign was to perform measurements of species concentrations, temperature and velocity in the incoming flow, and in the boundary and shock layers over a Thermal Protection System (TPS) model simulating a misalignment of tiles, by means of techniques developed by the plasma team from the University of Rouen. So, an original method using LIF diagnostic has been implemented to measure simultaneously the three parameters. Fluorescence of NO was induced in the high enthalpy air plasma flow by a tunable ArF-excimer laser via the ε-band system $D^2\Sigma^+_{(v'=0)} \leftarrow X^2\Pi_{(v''=1)}$. Measurements of the rotational temperature and NO number density have been performed. The spatial resolution of the LIF technique permitted accurate characterization of the boundary and shock layer, as well as shock thickness. Finally, flow velocity is deduced from the Doppler-shift measurements of excited rovibrational NOε band. Analysis of the results will allow to assess the validity of the computational tools in order to control the representativity of future industrial tests devoted to local aerodynamic studies.

1. INTRODUCTION

Re-entry trajectories for spacecrafts include large regions where the flow surrounding the vehicle is in high thermo-chemical non-equilibrium and behaves differently from a perfect gas. Molecules become vibrationally excited, dissociated and even ionized, and the hot gas may emit or absorb radiation. When the atoms produced by dissociation reach the wall surface, chemical reactions, including recombination, may occur. The thermo-chemical phenomena of vibration, dissociation, ionization, surface chemical reaction and radiation are referred to commonly as a high-temperature real-gas phenomena, and thus induce changes in the dynamic behavior of the flow and provide a strong and complex gas/surface interaction. To develop and verify phenomenological models, as well as to validate high enthalpy flows with CFD (Computed fluids Dynamics) tools, ground test facilities are required to generate such reacting gas flow over configurations of interest, and have to be implemented with sufficient diagnostics to describe the character and behavior of the flow. Although ground facilities have serious limitations in simulating full-scale flight conditions, they are capable of examining selected aspects which are expected to be vital to success in the full-scale flights, then offer the advantage of observations, such as optical flow visualization, which are not realistic in real flight.

Fine measurements in high enthalpy flows represent a technological challenge and research is done in this way to develop new methods and new instruments to probe the physical-chemical and aerodynamics states of re-entry plasmas. So, in the purpose of the framework of the Hermes program, to validate and improve CFD tools, experimental test cases has been planned on high enthalpy flows generated in different facilities of the Tsniimach Institute.

Paper presented at the RTO AVT Course on "Measurement Techniques for High Enthalpy and Plasma Flows", held in Rhode-Saint-Genèse, Belgium, 25-29 October 1999, and published in RTO EN-8.

In the test campaign conducted in the Tsniimach Center, Hermes flight conditions at altitude 50 km and Mach 15 has been covered in different continuous supersonic high enthalpy air flow ground test facilities. As real flight requirements are not fulfilled at the whole for chemistry and aerodynamic studies, the strategy adopted was to work on different facilities of which experimental conditions satisfy as much as possible the relevant problem of interest to validate and improve the numeric tools upon fixed flight conditions. The TT1 arc jet facility and a high frequency facility (Y13PHF-plasmatron) were devoted respectively to local aerodynamics problems arising in supersonic high temperature flow and physico-chemistry phenomena encountered in reactive-flow / surface interaction. The aim of the complete program was twofold. First, to improve reliable data for validation of chemical non-equilibrium shock and boundary layer and Navier-Stocke codes to compute a new test case of supersonic air-heated flow impinging on a TPS surface, and second to point out the potentiality of the LIF technique for instrumentation of continuous high enthalpy facilities.

The lecture is intend to present the LIF diagnostic tools developed for application to this specific study, to highlight its advantages and weaknesses, and to illustrate it with an experiment performed in an industrial environment. Before discussion on the experimental work is given, the general feature of the implemented facility and generalities on LIF measurements will be presented.

In the state of the art, the results presented here are drawn from LIF experiments performed on the TT1 arc jet facility for studies on the aerodynamic properties encountered in high temperature air flow impinging a shaped model designed for simulate a misalignment of tile. The ground test facility has been implemented by LIF technique to draw measurements of NO density, rotational temperature and velocity evolutions of the medium. Experiments are performed by means of a ArF-excimer laser in free jet as well as in numerous test sections within the boundary and shock layer down to the TPS surface model.

2. DIAGNOSTIC BASED ON LASER INDUCED FLUORSCENCE

2.1 Generality

The early development of Laser Induced Fluorescence (LIF) method was driven by single–point measurements, but application of LIF as non-intrusive method to probe complex flows in a short time exposure has been dominated by multi-point planar imaging. Planar Laser Induced Fluorescence (PLIF) may be considered as an advanced method of flow visualization. In common with methods such as Schlieren and Shadowgraph, the planar LIF is extremely used for quantitative and qualitative or semi-qualitative characterization of complex flow fields, providing spatially resolved information in a plane rather than integrated over a line-of-sight. The LIF has been extensively developed in the characterization of combustion processes and flames diagnostics for temperature and radical species measurements. The great capacity of LIF, which lies both to the strength of the fluorescence process and to the selectivity of species detection has demonstrated its applicability in high temperature medium under drastic pressure conditions associated with high enthalpy flow simulations. Well adapted to probe non-equilibrium airflow such as those generated in ground test facilities, LIF has become a powerful diagnostic tool for physico-chemical and aerodynamic property studies.

Laser Induced Fluorescence is the result of light emission incoming from an atom or a molecule excited by a laser beam. In a LIF measurement, the molecule is initially at its lower electronic state before it is excited to an upper electronic energy level by a laser source. When the beam is directed into the gas, the molecule absorbs a laser photon and undergoes transition from the populated electronic ground state to an upper electronic state of the absorbing species. The wavelength of the laser excitation needs to be tuned in coincidence with an absorption transition of the molecule of interest. Typically, the lower states probed are depending from the broadening of the excitation wavelength and correspond either to a single or to a set of rovibrational levels of the ground electronic state. Then, the originally upper populated states return to lower states of the ground state by radiative process in agreement with the selection rules and collisional processes, fluorescence and collisional quenching respectively.

The emitted fluorescence signal is detected at right angle from the incident laser beam pathway either onto a high-speed photo-multiplier (spot measurement) or a CCD intensified camera (1D or 2D planar measurement).

When the excitation wavelength of the laser could not be tuned on the absorption band of single species of a complex mixture, the selectivity of species can be done in detection, by tuning the spectral resolution through spectral filter (or monochromator), on the selected fluorescence signal of species of interest.

The fluorescence intensity provides information on the concentration of the emitting species. For quantitative interpretation of LIF experiment, a model involving the

population and competitive depopulation mechanisms is required.

In the following section, we will describe the basic physical processes involved in LIF experiment. First, a simplified two-level model will be presented, then extended to a multi-levels model. The second part will be devoted to the development of the method for simultaneous measurement of temperature, species concentration and velocity by LIF on NO in high enthalpy airflow. The calibration process associated will be presented to draw the absolute values of the measured flow properties. Finally, results from experiments on TT1 will be presented.

2.2 Simplified two level model

The two-level model illustrates the principal mechanisms involved in LIF of molecular species and allows to point out the important processes following its excitation by a monochromatic laser source. This model is a simplified one, and considers a single lower rovibrational level probed by the monochromatic radiation and the upper excited level populated by absorption and depopulated by spontaneous emission (fluorescence), stimulated emission and collisional quenching rate. The model doesn't take into account, neither the complete set of rotational levels involved by the selection rules at excitation, nor the complete fluorescence de-excitation observed from the upper excited vibrational level down to the various vibrational levels of the ground state.

Let us U_v, the spectral density energy of the incident laser radiation corresponding to a transition of the molecule, from the rovibrational level (E_1, N_1, v_1) of the lower electronic state to the rovibrational level (E_2, N_2, v_2) from the upper electronic excited state. Let us the total gas number density is given by $N_0=N_1+N_2$.

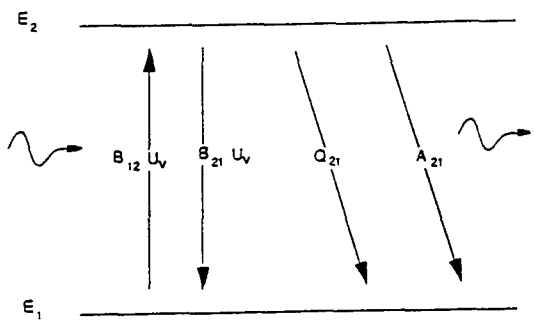

Fig(1): The two-level model

The dynamic to populate the upper excited state N_2 is driven as follow

- Absorption ($N_1B_{12}U_v$): the molecule absorbs a photon whose energy hv corresponds to the suitable transition E_2-E_1. Increasing of the N_2 population is proportional both to the N_1 population density of the lower state and to the laser intensity.
- Spontaneous emission (N_2A_{21}): the originally populated level N_2 return to the lower fundamental rovibrational state and light is emitted first at the same wavelength than the excitation laser radiation (resonant fluorescence).
- Stimulated emission ($N_2B_{21}U_v$): the molecule can be returned to its original quantum state by laser induced stimulated emission. This process is observed in the same direction as the light-of-sight of the incident laser beam, on the contrary to the spontaneous emission or fluorescence, which can be detected in the 4π steradians.
- Quenching (N_2Q_{21}): this non-radiative de-excitation process is imputed to the inelastic collisions with other molecules which results in electronic energy transfers between the different electronic states of the molecule.

The Einstein balance of population and de-population of the N_2 upper excited rovibrational level excited by laser radiation is expressed by the differential equation:

$$\frac{dN_2}{dt}=N_1B_{12}U_v-N_2B_{21}U_v-N_2(A_{21}-Q_{21}) \qquad (1)$$

A_{21}= Einstein coefficient for spontaneous emission (fluorescence emission)
B_{12}= Einstein coefficient for stimulated absorption
B_{21}= Einstein coefficient for stimulated emission
Q_{21}= the collisional transfer coefficient or quenching
U_v= the spectral energy density of the laser source
The Einstein balance includes the fluorescence emission and quenching terms, which depend from the selection rules existing between an excited rotational level (N_2) and the rotational levels of the ground state.

With assumption that at t=0 the N_2 level is not populated, and than $U_v(t)=Cte$, the solution of the differential equation is given as:

$$N_2(t)=\frac{N_1B_{12}U_v\left(1-e^{-((B_{12}+B_{21})U_v+A_{21}+Q_{21})t}\right)}{(B_{12}+B_{21})U_v+A_{21}+Q_{21}} \qquad (2)$$

Depending on the pulse laser intensity and in regard to the characteristic time τ, function of the intrinsic parameters of the molecule, the quenching rate and the energy density of the excitation source,

$$\tau=\left((B_{12}+B_{21})U_v+A_{21}+Q_{21}\right)^{-1} \qquad (3)$$

the equation of $N_2(t)$ can be rewritten as:

$$N_2(t) = N_1 B_{12} U_\nu \tau \left(1 - e^{-t/\tau}\right) \quad (4)$$

For the limiting case corresponding first to a low laser intensity or linear fluorescence regime given by

$$U_\nu \leq U_\nu^{sat} = \frac{A_{21} + Q_{21}}{B_{12} + B_{21}} \quad (5)$$

and assuming a pulse duration shorter than the characteristic time τ, the N_2 population can be considered as stationary and expressed as:

$$N_2 = N_1 B_{12} U_\nu \quad (6)$$

Finally, the fluorescence signal detected can be expressed as:

$$P_{21}^{fluo} = N_2 A_{21} \varepsilon_c V_c \frac{\Omega}{4\pi} h\nu \quad (7)$$

where ε_c, V_c, Ω_c are constants.
ε_c is a calibration constant, including the transmitivity characteristics of optics and the sensitivity of the detector, in the spectral range of the detection of interest.
V_c is the volume of gas probed by the laser.
Ω_c is the solid angle in collection.

From the measurement of the fluorescence signal and from knowledge of the emission probabilities of the emitting level considered, population of the upper excited level may be determined. With assumption of equilibrium at the temperature T, the Boltzmann equation will provide the total ground state population of the molecule.

The two-level model developed above is extended to the general analysis to express the fluorescence signal in different experimental situations, depending from the order of magnitude of the quenching term Q_{21} in regard to the Einstein coefficient for spontaneous emission A_{21}, and depending from the intensity and pulse laser duration. Because rotational energy transfer process (RET) acts to replenish the population of the laser excited states and at the opposite acts to drain the population from the laser-populated states to lower states, they have to be considered in the collisional quenching rate.

- In a weak energy density laser excitation with $(B_{12} + B_{21})U_\nu << A_{21} + Q_{21}$, the fluorescence emission is described simply with identical assumptions than the two-level model, and fluorescence emission simplifies to:

$$P^{fluo} \propto N_1 B_{12} U_\nu \frac{A_{12}}{A_{12} + Q_{12}}$$

If the quenching rate is in the same order of magnitude or greater than the radiative one, then it is possible to measure directly the temporal evolution of the fluorescence to extrapolate the quenching term. In the opposite, for to stronger quenching rate it had to be compared to the laser pulse duration.

2.3 Multi-levels model

For diatomic molecules, the simplified two-level model is not expected to be widely applicable to take into account the rotational and vibrational energy redistribution (RET and VET). Molecular models including three or four-levels have been developed to expressed the rapid coupling between rotational and also vibrational levels. However uncertainty persist in such model, because of lack of reliable data between levels involved in the fluorescence scheme of interest, and because quantitative detection of a single radical species by LIF therefore requires an enormous amount of information on collisions process. The RET and VET are generally approximated by a mean value averaged for a set of rotational and vibrational levels and more often compared to the electronic quenching term. Since the energy spacing between rotational and vibrational levels are closed to the translational energy of heavy particles, the RET and VET are more efficient than the electronic one, and remains the predominant process. Since the fast redistribution of the rovibronic levels between neighboring state takes place, the history of the excited level is lost in the fluorescence spectrum and lines are not necessary redistributed with a Boltzmann distribution.

The rotational (RET) and vibrational (VET) redistributions with neighbouring levels, in which inelastic collisions with the other molecules of the medium produce internal rotational and vibrational energy transfers of the molecule. We have to note that, the difficulty of LIF measurement remains in the absolute value determination of species density and is mainly imputed to this quenching term. Its value is highly depending from the collisional partners, temperature and pressure conditions, and is usually difficult to estimate and not well known for complex experimental working conditions.

In the model, the term of pre-dissociation, related to a change from a stable electronic state to a repulsive unstable one, has not been taken into account. Observed for some molecules excited with a high-energy laser source, the pre-dissociation is a non-radiative process, which can compete highly with the fluorescence emission. It is commonly imputed to interactions between atoms of the molecules with production of internal energy transfer following by the dissociation of the molecule. The molecules pass from an electronic excited state to the Continuum State of a neighbouring electronic state with the same or thermally accessible energy level. The pre-dissociation rate is shorter than the quenching rate. So, for a quantitative measurement of species concentration, it ids necessary to determine the quenching value.

2. 4 Quantitative measurements and calibration

The calibration of fluorescence signal to provide the absolute value of concentration is obtained by comparison between fluorescence light intensity of the molecule of interest and the Rayleigh scattering light recorded in a reference medium whose temperature and total density are well determined.

2.4.1 Rayleigh scattering

The fundamental principle governing the Rayleigh scattering is that the elastic collisions between gas molecules and incident laser light. The scattered light has the same wavelength as the incident light. The scattered light signal, in general, is directly proportional to the laser power, the gas density and a differential cross-section on the gas that is probed. For experiments with Rayleigh scattering detected at 90° in the direction perpendicular to the incident laser beam pathway and a minimized scattering volume defined by the intersection of the incident laser beam (polarized perpendicular to the detection) and the image of the aperture placed in front of the collection device, the Rayleigh scattering signal $P_{\nu_o}^{rayleigh}$ is given as:

$$P_{\nu_0}^{rayleigh} = (\varepsilon_c \Omega_c V_c) I_{\nu_0} N_{Ref} \sigma_{\nu_0}^{rayleigh} \quad (8)$$

with

- ε_c, V_c and Ω_c are calibration constant, respectively the efficiency of the collection device, the volume of gas probed by the laser and the solid angle in collection.
- $I_{\nu_0} = E_{\nu_0}^{laser}/S$ = incident laser intensity ($W.cm^{-2}$), expressed by the ratio of laser energy at ν_0 with section of the laser beam.
- N_{Ref} = $P\mathcal{A}_o/RT$, the total number density of the gas molecule (cm^{-3}) related to the pressure, temperature and Avogadro's number: $\mathcal{A}_o$=6.023 10^{23} molecules.mol^{-1}.

The term $\sigma^{rayleigh(\nu_0)}$ is the differential Rayleigh scattering cross section given by:

$$\sigma^{rayleigh(\nu_0)} = \left(\partial\sigma_{\nu_0}^{rayleigh}/\partial\Omega\right) = \frac{4\pi^2\nu^4}{c^4}\left(\frac{n-1}{N}\right)\sin^2\theta \quad (9)$$

with

- n = the real part of the refractive index of the gas.
- N = the molecular number density.
- θ = the scattering angle for detection

For a gas mixture, the formulation of the Rayleigh scattered cross section may be expressed as:

$$\sigma^{rayleigh(\nu_0)} = \sum_k \chi_k \sigma_{k,\nu_0}^{rayleigh} \quad (10)$$

with

- k the number of species present in the gas mixture.
- χ_k is the mole fraction of each species k ($\Sigma\chi_k$=1).
- $\sigma_{k,\nu_o}^{Rayleigh}$ its associated Rayleigh cross section.

2.4.2 Fluorescence de-excitation

In a complete radiative de-excitation scheme, it will be consider, first the summation on the numerous rovibrational levels involved by the selection rules at excitation then at de-excitation (rotational branches P, Q, R ...) which participate to the radiative de-excitation according to the allowed selection rules from the upper excited rovibrational state to a single ground rovibrational state), and second, the summation on the numerous vibrational levels involved (Δv=0,±1,2), from the upper excited vibrational level down to the numerous vibrational level of the ground state:

$$P_{total}^{fluo} = \sum_{\Delta v}\sum_{N_2}\sum_i P_{2i}^{fluo} \quad (11)$$

For most experiments and in presence of a gas mixture, different species or molecules may be excited at the same wavelength with the excitation source. The fluorescence resulting has to be filtered to allow a separate analysis of the different species present in the medium of interest. The use of a selective band-pass filter allows to limit the spectral range in detection to a single vibrational de-excitation corresponding to a selected molecule and then provide a selective analysis of the medium. For the molecule of interest, the intensity of fluorescence is then given as:

$$P_{\Delta v}^{fluo} = \sum_{N_2} P_{2i}^{fluo} \quad (12)$$

The ratio of $P_{total}^{fluo}/P_{\Delta v}^{fluo}$ is inversely proportional to the ratio of the vibrational emission probabilities between the vibrational level considered and all the vibrational levels participating to the global radiative de-excitation of the molecule of interest.

2.4.3 Fluorescence cross-section

In this section, let us consider only that the intensity of fluorescence is depending to a single rotational transition of the molecule, from the upper excited vibrational level to a single rovibrational i-level of the ground state.:

$$P_{2i}^{fluo} = \varepsilon_c V_c \frac{\Omega_c}{4\pi} h\nu N_2 A_{2i} \quad (13)$$

Considering the particular transition between the lower (E_1, N_1) and the upper (E_2, N_2) rotational leve, the absorption process induced by the laser radiation and expressed by the Einstein balance between the de-populated of lower rotational state and the populated upper rotational states is given by:

$$\left(\frac{dN_2}{dt}\right)^{abs} = N_1 B_{12} U_{\nu_{12}} \tag{14}$$

with $U_{\nu_{12}}$ the spectral density energy, so that $h\nu_{12} = E_2 - E_1$ and B_{12} the Einstein absorption coefficient of the transition considered.

With assumption of the drift movement of particles carry out with disorderly velocities and according a Maxwell velocity distribution, line are Doppler broadened and the cross section profile of the excited transition may be described by a gaussian shape such as:

$$\sigma_{12}^{abs} = \int_{\delta\nu_D} \sigma_{12}^{abs}(\nu)d\nu = \int_{\delta\nu_D} \sigma_{12}^{abs}(\nu_{12}) \exp\left(-4\ln 2\left(\frac{\nu-\nu_{12}}{\delta\nu_D}\right)^2\right) d\nu \tag{15}$$

$$= \sigma_{12}^{abs}(\nu_{12}) \left(\frac{\pi}{4\ln 2}\right)^{1/2} \delta\nu_D \tag{16}$$

with σ_{12}^{abs} the total absorption cross section, $\sigma_{12}^{abs}(\nu)$ the monochromatic absorption cross section, and $\sigma_{12}^{abs}(\nu_{12})$ the absorption cross section value on the center line. $\delta\nu_D$ is the Doppler broadening $\delta\nu_D = \nu_{12}\sqrt{\frac{8kT\ln 2}{mc^2}}$ and c is the speed of light.

Let us $U_{\nu_{12}} = Cte$, the spectral energy density of the radiative excitation, the differential equation related to the photon absorption process in the spectral range $\nu, \nu+\delta\nu$ can be expressed as:

$$\left[\frac{dN_2}{dt}\right]_{\nu+\delta\nu}^{abs} = \frac{cU_{\nu_{12}}}{h\nu} N_1 \sigma_{12}^{abs}(\nu) \frac{U_{\nu_{12}}}{h\nu} N_1 \tag{17}$$

With integration in the spectral range of ν, $\nu+\Delta\nu$ of the absorbing transition, the populated upper N_2-level by photon absorption can be rewritten as:

$$\left(\frac{dN_2}{dt}\right)^{abs} = \frac{cU_{\nu_{12}}}{h\nu} N_1 \sigma_{12}^{abs}(\nu_{12}) \left(\frac{\pi}{4\ln 2}\right)^{1/2} \delta\nu_D \tag{18}$$

The comparison with the Einstein balance equation thus provides the relationship between the absorption cross section and the Einstein coefficient for the transition of the molecule of interest:

$$\sigma_{12}^{abs}(\nu_{12}) = \frac{h\nu_{12}}{c} B_{12} \left(\frac{4\ln 2}{\pi}\right)^{1/2} \frac{1}{\delta\nu_D} \tag{19}$$

From relations between Einstein coefficients and degeneracy between the two levels involved in the transition:

$$B_{12} = \frac{\varpi_2}{\varpi_1} B_{21} = \frac{\varpi_2}{\varpi_1} \frac{c^3}{8\pi h\nu_{12}^3} A_{21} \tag{20}$$

Finally, the absorption cross section is expressed as:

$$\sigma_{12}^{abs}(\nu_{12}) = \frac{\varpi_2}{\varpi_1} \frac{c^3}{\nu_{12}^3} A_{21} \left(\frac{1}{4\pi^2}\right) \sqrt{\frac{m}{8kT}} \tag{21}$$

2.4.4 Calibration method

The calibration method for absolute concentration measurement is provided by the ratio of the intensity of fluorescence of the molecule probed with the Rayleigh intensity of a reference gas mixture probed in the same experimental condition. Both measurement is performed assuming , a given operating condition for the exciting source and identical optical setup and detection device. With such operating conditions, the incident laser radiation I_{λ_0}, the transmitivity of optical setup ε_c, and the size and probed volume $V_c\Omega_c$ are constants, and are ruled out in the expression of the ratio of fluorescence with Rayleigh given by:

$$\frac{P_{21}^{fluo}}{P^{rayleigh(\nu_0)}} = \frac{\alpha N_1 \sigma_{21}^{fluo}}{N_{Ref}\sigma^{rayleigh(\nu_0)}}$$

The ratio $P_{21}^{fluo}/P^{rayleigh(\nu_0)}$ is experimentally measured. The term $N_{Ref}\sigma^{rayleigh(\nu_0)}$ is calculated for the calibration medium used as the reference medium. The term σ_{21}^{fluo} is the fluorescence cross section and can be calculated easily from the absorption cross section term. N_1 is the unknown parameter to determine. The term α is a constant.

The variations of the Rayleigh scattered light signal are the result of the mixture number density (i.e. the variation of temperature or pressure or both) or the species variations, or even both. Hence, an unambiguous interpretation of the Rayleigh scattered light signal requires that experiment has to be conducted in reference mixture for which the term $N_{Ref}\sigma^{rayleigh(\nu_0)}$ is well known. The ratio of intensities given above is expressed for a single transition and a monochromatic detection. Depending on the spectral range at excitation and detection of fluorescence, the term $N_1\sigma_{21}^{fluo}$ have to be summed on all the rovibronic considered.

2.5 Temperature measurement with LIF

With density measurement, the temperature is one of most important flow parameters to be determined for simulation of kinetic processes with numerical models and comparisons between model predictions and experimental test case. One of the advantages of LIF is that measurement of number density and temperature may be performed together with the same spatial resolution at the location of the measurement point.

The rotational temperature is determined from the relative intensity of less two rotational lines within a molecular band with assumption of Boltzmann equilibrium. At the opposite of number density measurement, the temperature value is drawn from comparison of the relative experimental lines ratio with the calculated one by means of synthetic spectra computed at different temperatures. For lines recorded with the same operating experimental conditions, no information on the size of the probed volume and detection solid angle are to be known. Accuracy of the measurement will be provided by accuracy of the synthetic spectrum, the knowledge of the exact excitation laser radiation, the lines involved in the fluorescence process (energy spacing between rotational level, transition probability, quantum yield...) and spectral range in detection. Whatever the excitation source used, the two levels model presented above has to be completed to include the selection rules between the rovibrational levels involved at excitation and de-excitation, to take into account the possible overlapping of lines.

For two levels involved, the temperature is drawn from the ratio of the relative intensity of the two lines, but for several lines involved, more accuracy can be obtained from the semi-logarithmic Boltzmann plot of fluorescence intensity weighted by the Einstein transition probability P_k and degeneracy g_k of the considered k levels, versus its energy E_k:

$$Ln\left(\frac{\phi_{fluo}}{P_k g_k}\right) = -\left(\frac{E_k}{kT}\right) + Cte$$

The accuracy on the temperature value will depend first, on the energy spacing between the rotational levels involves and on the relative rovibronic population in regard to the medium temperature. Secondary, it will depend on the radiative process observed in detection: i.e. either radiation from an excitation spectrum or from a fluorescence spectrum.

For a broadband laser excitation (i.e. fluorescence spectrum), numerous rovibronic transitions are simultaneously excited from the low energy states to the upper excited one according to the selection rules of individual excited transition. The lines intensity ratio is drawn from the fluorescence spectrum spectrally resolved through a high resolving monochromator set at a selective Δv vibrational fluorescence de-excitation. By this way, the temperature is measured from the upper excited state and is greatly dependant from the population equilibrium of this level by the RET process. Accuracy on the temperature will then depend on the efficiency of the RET to provide a Boltzmann distribution on the upper excited.

The use of a single laser source working in broadband at excitation and coupled in detection with a monochromator and a CCD camera allows to perform a 1D-temperature measurement on a light of sight of the laser beam if assumption of efficient RET is done. The 2D description of the CCD camera is thus devoted, in one direction along the beam pathway for the spatial resolution of the medium, and in the second direction for the spectral resolution through the monochromator.

For a narrow band excitation (excitation spectrum), the laser is tuned separately on the maximum peak intensity of each rovibronic transition of interest and thus provides the spectral resolution at excitation. In detection an excitation spectrum is recorded for both rovibronic transition considered. Without filtering, the complete radiative de-excitation depends only on the lower rovibronic state excited by the laser radiation, and thus on the population equilibrium of the ground state.

In case of short run duration of the test facilities, the two-line thermometry is used to probe simultaneously the maximum intensity of two rotational lines from the same excited vibrational level. This method is commonly used for planar temperature field determination with a CCD camera (or for spot temperature measurement with two photo-multipliers tuned on each line). However and as a general rule, it required to focus at the same location two planar laser beams tuned respectively on the maximum peak intensity of each transition of interest, with an identical energy density. Accuracy on the temperature determination thus depends mainly from accuracy of the excitation wavelength in regard to the rovibrational lines selected. In the case of weak or strong laser excitation (non-saturated or saturated LIF), the fluorescence signal is solely dependant from the initial-ground state populations which may be assumed as function of the temperature alone (i.e. ground state populated with a Boltzmann distribution). In the intermediate case, between weak and strong laser excitation, the transitions are only partially saturated and uncertainties on temperature may provide from the ratio of intensity.

The detection limit of a photo-multiplier being in some order of magnitude lower than the detection limit of a CCD camera, the use of a single spot measurement is preferred in medium with low absorbing properties or with low number density. Add to the wish to increase the signal to noise ratio, the single spot LIF is commonly used, when difficult experimental geometry conditions doesn't allow to implement the ground test facility or the medium with planar diagnostic. This implies that, for short run duration of the facility or non-continuous flow, the temperature measurement can be achieved with two wavelength excitations. For continuous facility, the problem is less drastic. With assumption that the medium is in stationary state, the use of a single excitation laser source may be conceivable. Here, the temperature measurement is obtained from an excitation spectrum. The excitation wavelength of the laser is tuned twice, respectively on each of two absorbing transitions considered and ratio of line intensities drawn from the excitation spectrum recorded through a spectral band-pass filter set at a fixed Δv vibrational de-excitation sequence. As it has been noted here above, accuracy on the maximum peak intensity determination will depend essentially from the accuracy of the excitation wavelength spectral tuning. As it is not so easier to scale the maximum peak intensity of the monochromatic exciting radiation together with the absorbing line, the two absorbing lines chosen for the ratio will be both spectrally described by tuning the laser radiation over entire spectral range corresponding to the line profiles. Although the recording time necessary to perform the temperature measurement by this way is greater than the time needed to performed experiment with two laser sources (set at the two wavelengths), this method remains well adapted to the temperature measurement in stationary medium generated by continuous facilities.

2.6 Velocity measurement with LIF

The narrow band radiation of the exciting laser source can be devoted to evaluate the flow velocity via the Doppler shift of the highly resolved excitation spectrum.

In this section we consider emitting molecules excited by the laser radiation and a Maxwell velocity distribution of emitting species which move with a the mean velocity of the flow. The light emitted from species and observed along a line of sight different from the direction of the flow, is shifted by the quantity corresponding to the mean velocity component of the molecule in the direction of observation. For observation in the direction of the particle mean velocity, the light emitted (or line profile) is blue-shifted. Conversely, it is red-shifted with the same absolute shift value for observation in the direction opposite to the mean movement of the flow stream. For observation perpendicularly to the flow axis, the light emitted is unshifted. The shift in wavelength is given as the Doppler shift and expressed as:

$$\frac{\Delta v}{v} = \frac{v}{c}\cos\theta$$

where v is the frequency, v the velocity and c the light speed. θ is the difference angle between the flow axis and the light of sight of observation in a direction such as $0<\theta<\pi/2$. Experiment may be carried out when the laser is spectrally wider than the probed line and requires high resolution in detection, thus damageable for the signal detection. With a monochromatic excitation, it is preferred to resolve the line by absorption.

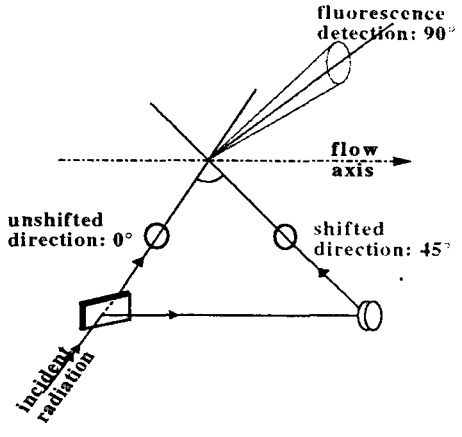

Fig(2): velocity measurement

Let us the flow excited with a laser radiation in the two excitation pathways, respectively in the direction 0° normal to the flow axis (unshifted line) and in the direction 45° upward the flow axis (shift line). In the direction 0°, the molecule will be excited if the laser excitation frequency coincides exactly to a rovibronic transition of the molecule. In the direction 45°, the molecule will be excited if the laser excitation frequency is shifted from the quantity corresponding to the Doppler shift. So, with two successive excitation pathways (0° and 45°) and a monochromatic excitation tilted on a spectral range corresponding to the Doppler shift, since the whole fluorescence signal is proportional to the monochromatic absorption coefficient.

3. NO_ε SYNTHETIC SPECTRUM

Synthetic spectrum of the NO ε-band is computed to carry out information on lines distribution and lines intensity. These information complete the experimental basis work necessary to tilt the excitation laser radiation on lines of interest and also necessary for the temperature

determination in case of lines are not sufficient resolved, and than the overlapping of rovibrational lines may provide uncertainties on lines ratio measurement.

The fluorescence intensity distribution observed depends on the rotational levels involved first at excitation by the spectral distribution of the incident light, and second on the detection by the spectral range analyzed.

The excimer excitation source avoids simultaneous excitation of numerous rovibrational levels, depending first on the narrow or broad-band excitation and second, depending from the selection rules between the rovibrational levels involved at excitation, from the electronic ground state of NO ε-band $X^2\Pi_{(v''=1)}$ to the upper electronic state $D^2\Sigma^+_{(v'=0)}$. The upper state belongs to the Hund's case b, the lower state is a Hund's case a, with a spin orbit coupling constant. Each of the two sub-bands consists of twelve branches, whose the P, Q, R, ^PQ, ^QR and ^RP are the major ones, well separated for low rovibrational levels but merged for higher rotational numbers.

The selective absorption cross sections of the rovibrational transitions are computed in the spectral range of the exciting source, just as fairly from a discret excitation and absorption molecular spectrum of NO. Thus, absorption spectrum is computed assuming a Doppler broadening for the rovibrational lines (low pressure conditions of the experiment) , the experimental energy distribution of the exciting source which includes the intensity gaps resulting from the O_2 Schumann-Runge absorption band in the spectral range of the laser at 193.1, 193.3, 193.5, 193.7 nm and geometric factors corresponding to apparatus function of the optical arrangement. Calculation is done assuming for the population number density of the ground state $X^2\Pi_{(v''=1)}$, a Boltzmann distribution at the rotational temperature. Finally, the absorption spectrum provides the number density of the particles absorbed and then the relative population number density of the numerous rotational levels of the upper state $D^2\Sigma^+_{(v'=0)}$, populated from the $X^2\Pi_{(v''=1)}$ state by the incident laser radiation.

The fluorescence associated to the radiative de-excitation from the upper $D^2\Sigma^+_{(v'=0)}$ state to the ground state $X^2\Pi$ is also computed accurately. This radiative de-excitation includes the radiative cascading process between rovibrational levels from the upper state $D^2\Sigma^+_{(v'=0)}$, down to the numerous vibrational levels of the ground state which satisfied the selection rule $\Delta v=0, 1, 2....$ The fluorescence cross section is calculated line by line for all the transitions observed and selected in detection through a spectral filter. Finally, an averaged fluorescence cross section value is calculated for the whole rotational transitions considered and will be used for an absolute calibration of the NO number density.

4. MODEL DESIGN AND FLOW CONDITIONS

Because of the high enthalpy levels required, the difficulties to reproduce high-speed flight conditions in wind tunnel are increasing. With the non-equilibrium flow conditions expected, analysis implies to test full-scale models. In regard to these working conditions, the TT1 facility (fig.*) is well adapted with its large experimental test section, its high enthalpy and air mass-flow rates.

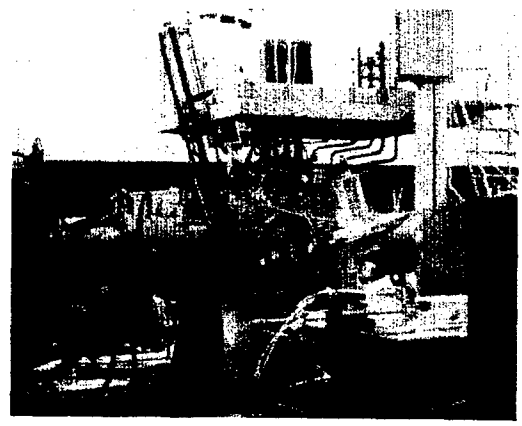

The air plasma source is a classical D.C. arc jet with a classical electrode configuration. The arc is generated between the tip of a copper cathode and a cylindrical anode corresponding to the convergent part of the reservoir chamber. Expanding high enthalpy gas through a water-cooled convergent-divergent nozzle generates the supersonic flow, before expansion in the low-pressure experimental test chamber set at 10^3 Pa. The well-shaped divergent part of the nozzle has been calculated to provide a homogeneous air plasma flow at Mach 4.5, over the entire section of the nozzle exit of about 300 mm wide.

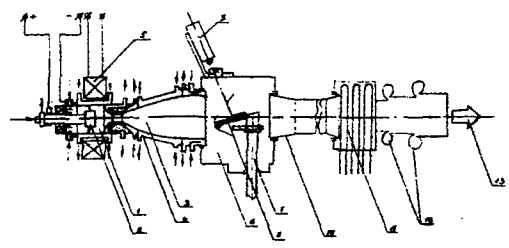

Fig(3): TT1 wind tunnel

The flow conditions in the stagnation chamber are $P_o \approx 1.6\ 10^5$ Pa, $H_o \approx 6.3$ MJ/kg and $T_o \approx 4100$ K with an input electric power supply of about 4 MW and an airflow rate of 0.5 kg/sec. The test conditions of the four runs retained in the test campaign to validate and improve CFD tools are summarized in Table 1.

At the nozzle outlet, the enthalpy leads to a thermo-chemical non-equilibrium flow. The pressure and temperature is estimated of about 2 10^4 Pa and 1000 K with a Reynolds number of $Re_{unit}=10^6$. The enthalpy leads to a supersonic vibrationaly excited, weakly dissociated and even ionized air plasma flow.

		Test run	#1	#2	#3	#4
T_0	°K	hot gas stagnation heater	4100	4159	4117.7	3910
P_0	$kg.cm^{-2}$	hot gas pressure heater	6.991	7.114	7.079	7.100
P_{02}	$kg.cm^{-2}$	cold gas pressure heater	1.640	1.642	1.637	1.697
M_s		Mach number	4.913	4.691	4.762	4.867
V	$m.s^{-1}$	Velocity nozzle exit	3143.5	3345.9	3332.5	3205.4
R_e	m^{-1}	Reynolds number	121823	101498	98579.3	114805
G	kg.s	Mass flow rate	.514	.497	.495	.513
P_1	$kg.cm^{-2}$	Static P test chamber	.006	.007	.006	.006
H_1	$kcal.kg^{-1}$	Static enthalpy	263.3	361.8	342.8	287.3
H_0	$kcal.kg^{-1}$	Total enthalpy	1443.6	1699.1	1669.3	1514.6
W	MWatt	Heater total power	3.813	3.959	3.941	4.002
P_{01}	$kg.cm^{-2}$	Stagnation Pshock	.180	.191	.177	.180
M_1	$kg.c.m^{-2}$	Gas viscosity flow	-	-	-	-
T_{01}	°K	Static T	920.3	1221.4	1163.3	993.6
R_{01}	$g.c^2.m^{-4}$	Gas density nozzle exit	.182	.167	.158	.175

Table 1: TT1 wind tunnel conditions

Add to the main characteristics of such facility is the long duration of the runs which can be maintain up to 15 minutes and thus allow to performed numerous tests during one run with unchanged operating conditions. In comparison with tests performed during short runs as in shock tube, the long run of TT1 facility makes easier implementation of continuous diagnostic as the LIF method developed for this specific test campaign.

Aerodynamics studies are performed radialy in the free stream, 190 mm downstream from the nozzle exit, then in numerous sections of the shock layer developed around a TPS model simulating a misalignment of tiles. In regard to the real flight conditions and to the difficulty to transpose the size and the shape of the tiles overlapping to a resized model dedicated for testing in experimental ground test facility, the used of a full-scaled model has been chosen. So, in such experimental situation, the huge diameter (300 mm in diameter) of the TT1 plasma flow is well adapted and representative of the test case of interest.

The model is made of insulating material like BOURAN (mainly SiO_2)and it looks like to a flat plate 200 mm length and 100 mm spanwidth, with a step of 3 mm height located 100 mm downstream from the blunt leading edge (Fig.*). The model is aligned on the jet axis with a 15 degrees incidence to reproduce the required parietal heat flux conditions. Most critical seems to be the high temperature expected on the leading edge, so it as been proposed to build the leading edge as a water-cooled copper cylinder of 20 mm radius.

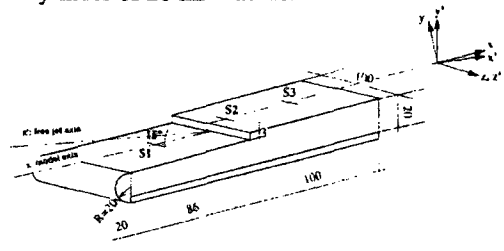

Fig(4): The SiO_2 model

5. EXPERIMENT DESCRIPTION

This paper deals with the experiments achieved in the TT1 wind tunnel. The small changes in the heater total power, the mass flow rate, the stagnation pressure in the heater and the static pressure in the test chamber provide weak changes of experimental working conditions for each run, despite efforts to maintains identical test conditions from run to run. The challenge of this test campaign was then to perform in the duration of each run sufficient measurements in the flow field (without then in presence of the model), to provide the best description of the flow parameters related to a particular test condition.

The two excitation mode of the ArF excimer source are used. The plasma flow is first implemented in broad-band mode to provides signing of species and information on the thickness evolution of the shock layer from the bow shock up the step of the model. In narrow band mode, the laser is tuned to excite single rovibrational levels of NO molecule. These experiments are devoted to the measurement of NO number density and temperature. Finally, the high resolved excitation spectra is used to determine the flow velocity via the Doppler shift of excitation lines.

An accurate description of the flow parameters has been allowed by the original LIF methodology developed for the test campaign on the High enthalpy air flow TT1. It consists in measuring simultaneously the number density, temperature and velocity using Laser Induced Fluorescence on NOε-band $D^2\Sigma^+_{(v'=0)} \leftarrow X^2\Sigma^+_{(v''=1)}$. Briefly, the number density will measured from line intensity after calibration of the fluorescence intensity with a reference medium. The temperature will be drawn from the ratio of two lines intensity after comparison with a computed fluorescence

spectrum (including the experimental optical arrangement, essentially the laser emission and optical apparatus functions). The velocity will be determined by tilting the monochromatic excitation line of the laser over the spectral range corresponding to the Doppler effect.

It is so required that the ArF laser have first, to excite the NO-molecule to resolve first, the rovibrational lines structure of the NOε-spectrum and second, to describe the Doppler shifted effect resulting from an excitation of the plasma flow in a direction along the line-of-side of the drift movement of the flow stream

In order to provide simultaneously the three parameters, the working conditions for excimer laser excitation and fluorescence detection have to satisfy some requirements listed hereafter:

1- Number density will be measured with a narrow band mode excitation centered on the center line of a NO-rovibrational line well identified. So an accurate scaling of the excitation wavelength of the laser is needed and will be provided by the 50mbar NO-reference cell. Experimental data on lines positions will be used first for experiment and second, to adjust lines positions of the NOε synthetic spectra in order to provide an accurate tool of comparison for simulation. It is note here that methodology carried out for the temperature measurement (next part) is based on the accuracy of line position and even on overlapping of lines, and thus need the used of a well representative synthetic spectrum to provide the expected accuracy on the temperature measurement. The absolute concentration value for NO will be drawn from calibration of the Rayleigh light intensity measured in a well known medium (air STP for example) with the same operating condition (laser power, probe volume and solid angle in detection and detection device).

2- Temperature will be drawn from the ratio of two lines intensity at their maximum intensity (center line of each transition considered). The NOε-synthetic spectrum allows to select the transitions of interest in the spectral range of the narrow-band excimer excitation. The rovibrational transitions have to be close to each other (low energy spacing between the lines) to limit the tilting of the laser between the lines and then to limit the time of measurement. Accurate measurement will be obtained with an accurate positioning of the excitation wavelength on the center line of the two or group of rovibrational levels chosen. In order to increase the accuracy of measurement, the two rovibrational transitions considered have to satisfy the following criteria: one of the two transitions considered have to be greatly dependent with the temperature in the range of interest (500-2000 K), and the other one without dependence (unit line intensity). The choice of the better transitions which satisfied these requirements are driven according to the evolutions observed from computed spectra.

3- Velocity measurement will be provided by the shift in wavelength at excitation and not by the shift observed at detection. Considering the two excitation pathways of the optical arrangement (named respectively the unshifted or 0°incidence and unshifted or 45°incidence), the fluorescence detection of a single rovibrational level would be observed at a only one wavelength if, the wavelength between the two excitation pathways is tuned at excitation by the amount corresponding to the Doppler shift value. The Doppler shift value is proportional to the velocity of the medium probed following the two particularly excitation pathways. The lower limit of the Doppler shift value is estimated to 1.8 10^{-4}nm and corresponds to a velocity of about 300 $m.s^{-1}$ in the air plasma flow (accuracy is given by the step by step increment of the excitation wavelength)

4- In addition to these requirements, the fluorescence detection has to be tuned on the more intense vibrational fluorescence de-excitation, except the resonant one, in order to rule out reflection and Rayleigh scattering. It is also required nor overlapping with the O_2 Schumann-Runge band, neither other band systems (excited by the laser or observed from plasma emission). For calibration of number density and velocity, the operating conditions have to be maintained constant for each measurement point (excitation pathways, probed volume, laser intensity, and so on ...).

Before implementation of the TT1 facility, some experiments were conducted in a high frequency plasmatron of the TSNIIMACH (Y13PHF) to improve the methodology and record reliable data on the rovibrational structure of the NOε-band, and particularly to calibrate the energy level (or lines position) of the NOε-rovibrational lines in regard to the reference lines of the well known NO_β system $B^2\Pi_{(v'=7)} \leftarrow X^2\Pi^+_{(v''=0)}$.

6. EXPERIMENTAL ARRANGEMENT

5.1 The laser source

A tunable ArF excimer laser (Lambda Physik LPX 150/T) is used to induce fluorescence of NO-molecule in the high enthalpy airflow of the TT1 facility. With an excitation at 193.4 nm, the excitation source is tuned on the rovibrational lines of the ε-band $D^2\Sigma^+_{(v'=0)} \leftarrow X^2\Sigma^+_{(v''=1)}$.

The excimer laser consists of two separate cavities to work independently in broadband mode or narrow band-mode. The broadband radiation is centered at 193.4 nm with a 0.5 nm FWHM. In narrow band-mode, the 1.2 10^{-3} nm FWHM pulsed radiation can be tuned with a step increment of 2.2 10^{-4} nm on the full spectral range of the broadband ArF emission. A 10 ns pulse is achieved up to 120 mJ/pulse energy and a 1-50 Hz repetition rate.

In narrow-band mode, the excimer laser has to be calibrated in wavelength to be tuned on the wavelength of interest. Thus, a weak part of the laser radiation is directed in an external reference source made of a home-made static cell filled with 50 mbar of pure NO at 300K. In these operating conditions the calibration cell allows to provide the excitation spectrum of the NO_β system $B^2\Pi_{(v'=7)} \leftarrow X^2\Pi^+_{(v''=0)}$ whose lines are well identified. From the good knowledge of the β-lines wavelengths, the correspondence between the excitation wavelength and the tilting of the ArF grating (which selects the monochromatic excitation radiation) is provided with accuracy (1.2 10^{-3} nm).

A pin silicon photocell (Hamamatsu S1722-02) is added at the laser source exit to correct the pulse to pulse energy variations of the laser.

5.2 Setup and optical arrangement

The TPS model designed to simulate a misalignment of tiles is immersed in the flow stream, its blunt leading edge centered on the jet axis and its surface set at 15°deg upward. It is fixed on a 1D displacement and may be translated during the run, by step of 10 mm in the direction of the jet axis. This device allows to analyze numerous test sections in the shock layer from the bow shock to the step, during a single run.

A scheme of the experimental setup is depicted in Fig(*). The optical setup consists of the laser, its reference cell (filled with 50 mbar of NO) and dielectric high reflection coating mirrors set to direct the laser beam in the test chamber. An optical periscope is fastened by a stepper motor with accuracy of 10 μm and directed 15° downward the vertical direction. It is equipped with a beamsplitter to divide the excitation beam in two excitation beams, one for the unshifted excitation, the second one for the shifted excitation. The two preferential pathways for Doppler shift measurement are respectively at 0° and 45°deg incidence in regard to the flow axis. The velocity or Doppler shift measurement is performed by recording first the unshifted line, the shifted pathway being close. When the maximum line intensity is recorded, the shifted pathway is closed and the unshifted one automatically open.

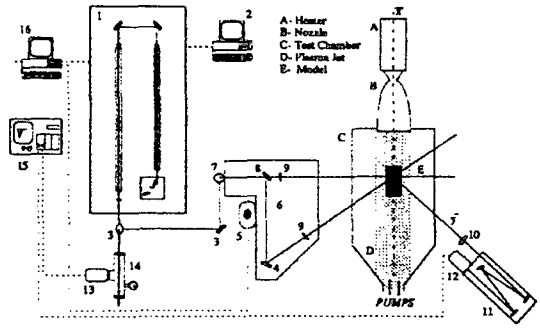

Fig(5): Optical setup

1- laser, 2- PC control, 3- 90°mirror, 4- 45°mirror, 5- vertical translation, 6- optical table, 7-optical periscope, 8-beam splitter, 9-lens, 10-focalisation lens, 11-spectrometer, 12-photomultiplier, 13- photomultiplier, 14- numerical oscilloscope, 15- PC control

The free jet radial and shock layer analysis perpendicularly to the surface of the model are carried out by translation of this optical arrangement (focussing lens, beamsplitter and mirrors) set on the 1D displacement device. Whatever is the altitude probed in the test of interest, the crossing point of the two excitation pathways always coincides and the probe excitation volume is maintains constant. In the directions where the most significant gradients are expected. Fine spatial resolution down to 200 μm is achieved with the focussing lenses f1000 mm (radially in the free jet and normal to the surface of the model).

The test chamber (1m*1m*1m) is equipped with tree optical access. Their location is forced first, by the incidence of the model aligned 15° upward the jet axis, and second, by the method of Doppler shift measurement used. For detection of fluorescence, the top of test chamber is equipped by an optical window, UV-fused silica 100 mm in diameter. To induce fluorescence, two optical access are set on the side part of the test chamber to provide the two excitation pathways for Doppler shift measurement. The first one is centered on the jet axis, at 190 mm from the nozzle exit. It allows the laser to enter the test chamber perpendicularly to the flow axis and to provide the orthogonal access required for the unshifted Doppler measurement. The shifted measurement is provided by the second window set at 15° upward the free jet axis and 45° incidence from the previous optical window. Its positioning in regard to the previous one allows to cross the shifted excitation pathway with the unshifted excitation pathway in the free jet section of interest defined at 190 mm from the nozzle exit. Optical access at excitation are limited by

the size of the windows (UV fused silica, 100 mm in diameter) and allow analysis of the flow stream 50 mm on either side.

The fluorescence signal is collected on the top of the test chamber, at right angle from the two-excitation beam pathways. The signal is recorded through a monochromator used as a spectral filter (Jobin-Yvon, f588 mm, 3600 groves/mm holographic UV grating), onto a UV sensitive photomultiplier (RTC XP2020Q). The probe volume is imaged with a f50 mm fused silica lens onto the entrance slit (600 μm) of the monochromator used as a tuning 0.4 nm FWHM band-pass filter. Because the detection device is fixed (and couldn't be displaced), the solid angle in collection have not to be too large in order to make assumption that the measurement volume is unchanged when the focussing point of both excitation pathways are displaced across the entire section of the flow stream.

The time resolved fluorescence is detected in the plasma flow and in the reference cell, then recorded on a 2 GHz numerical oscilloscope (Tektronic DSA 602A). Data are transferred to a PC computer simultaneously with information on the laser intensity of the incident pulse monitored via a power-meter and positioning of the measurement point provided by the optical periscope device.

The experimental setup as the whole (optical periscope, monochromator, detection device and the excimer laser) are fully automated and are operated under remote control. During the run, the NO reference cell provides the accurate positioning in wavelength of the laser which can be tilted on the wavelength of interest. The location of the measurement point which can be adjusted as well as the positioning of the model along the jet axis. In detection, the spectral range for fluorescence detection can be adapted to the spectral range of interest.

7. OPERATING CONDITIONS

7.1 Introduction and positioning of the model

At the ignition of the wind tunnel, the model is removed to avoid impact with metallic particles coming from electrodes erosion and maintains apart from the flow as long as the input power, gas flow rate and static pressure in the test chamber are not set to their nominal value. When the working conditions are reached, the model is immersed in the flow at its nominal position, so that its rounded leading edge is located on the jet axis, at a distance of 190 mm from the nozzle exit. The surface is 15° upward the jet axis.

To perform measurements in a given section, the model is displaced parallel to the flow axis by step increment of 10 mm, up to that the section of interest coincide with the optical direction defined by the incident laser beam pathways, oriented perpendicularly to the flow axis. Measurements in the section perpendicularly to the surface of the model will be provide by the optical periscope 1D-displacement, with step increment down to 10 μm.

7.2 Operating conditions for LIF diagnostic

The huge span width of the model coupled with the solid angle of the input laser excitation and the size of the laser spot doesn't allow to focus the laser down to 1 mm from the surface of the model whitout increase a parasite reflection damageable to the fluorescence signal. Thus no data have to be considered in the last millimeter over the model, and no measurement will be possible at the foot of the step of the model. The reflection provides a high level of light emission centered at the excitation wavelength which can be rule out from fluorescence emission, except if a narrow band-pass filter is set in detection on a vibrational sequence of the complete fluorescence radiative de-excitation different from the resonant fluorescence .

Before to start the run, the detection is tuned on the excitation wavelength to record the signal issued from the reflection of the laser on the model, and to determine the absolute location of the model, first in the flow and second, location of its surface in regard to the reference position of the 1D-displacement of the optical periscope.

When the model is immersed in the flow, the Infra-red record points out that 60 seconds are necessary to reach a thermo-equilibrium of its surface (up to 95%). LIF will be carried out after this delay time.

The long run duration (15 mn) is convenient to multiply points of measurement. Notably in experiments with the model, the long run allow to probe the free flow before to introduce the model and then, to provide with the identical experimental working condition of the wind tunnel, both data set from the flow and from the shock layer .

7.3 Data acquisition

(see §8.2 : Transitions for the simultaneous measurements of number density, temperature and velocity)

Considering first, the criteria retained for the simultaneous measurement of number density, temperature and velocity and second, the long duration of the run, the LIF experiments are conducted as follow:

a) Fluorescence is filtered in detection. The filter is a narrow band one, but can be consider as a broadband filter in regard to the number of rovibrational lines involved in the narrow band mode excitation. Thus, shifted and unshifted lines will be detected.

b) The first fluorescence record is to determine the spectral spacing between the reference βNO line (R_2(30.5) measured in the reference NO-cell, and the ε-NO line Q_1(31.5) measured in the air plasma flow with the unshifted beam pathway (0°). The laser radiation is tuned over the entire exact spectral range of the reference βNO line (R_2(30.5) and the ε-NO line Q_1(31.5), then stopped.

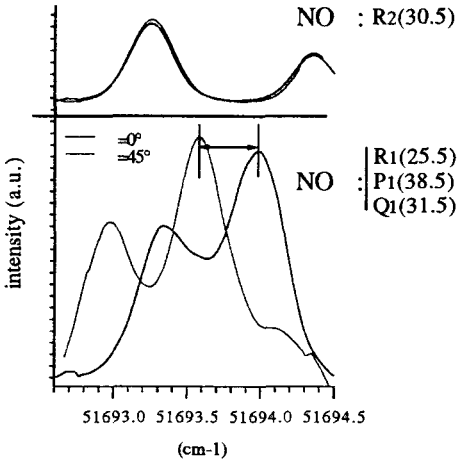

Fig(6): Doppler shift measurement

c) The second fluorescence records is carried out with the shifted excitation beam pathway set at 45°deg incidence. The laser radiation is tuned over the βNO line (R_2(30.5) used always as the common reference line and over the ε-NO lines P_1(38.5), R_1(25.5), Q_1(31.5) previously determined. For this record, the spectral spacing of the record will be identical to the previous one but spectral range to consider has to be brought forward to take into account the Doppler shift effect

d) The velocity will be drawn from the spectral spacing measured with the two records between the NOβ line (R_2(30.5) and the NOε line Q_1(31.5).

The temperature will be drawn from the ratio intensity of the lines from the group of NOε lines after comparison with synthetic spectra.
The integrated fluorescence intensity will provide the absolute number density, after calibration by intensity of Rayleigh scattering.

8. LIF MEASUREMENTS

8.1 The resolved NOε spectrum

A high enthalpy air flow generated in the high frequency plasmatron Y13PHF of the TSNIIMACH has been implemented in order to provide reliable data on the NOε spectrum. The working conditions of such facility in which the plasma is generated in a quartz tube without electrode, thus provides a flow without impurity. In addition, the stability and reproducible flow has been verified and provides a convenient high enthalpy air plasma source for basis experimental.

The NO fluorescence is induced in the air plasma flow by pumping the $D^2\Sigma^+_{(v'=0)} \leftarrow X^2\Sigma^+_{(v''=1)}$ ε-band with the incident ArF laser radiation tuned in narrow-band mode on the ArF tuning wavelength range from 192.8 to 193.8 nm. The fluorescence emission is collected through the monochromator from the (0-2) vibrational band (198 to 202 nm). The only excitation spectrum observed is the NOε band system, via the $D^2\Sigma^+_{(v'=0)} \leftarrow X^2\Sigma^+_{(v''=1)}$ excitation scheme. Nor rovibronic transition from the hot Schumann Runge lines, neither the γ-NO band $A^2\Sigma^+ \leftarrow X^2\Pi$ (3-0) and (4-1) are observed. The radiative fluorescence is detected at right angle from the straight line of the incident beam is recorded through a monochromator used as a broad-band filter. The spatial resolution is minimized in order to provide a probe volume in which the density and temperature evolutions are expected to be constant. From analysis of fluorescence emission at different height in the section of the plasma flow, the line intensity with the temperature dependence may be observed on the records.

8.2 Transitions for the simultaneous measurements of number density, temperature and velocity

The spectrum presented fig* is described by the P, Q and R-branches of the NOε band $D^2\Sigma^+_{(v'=0)} \leftarrow X^2\Sigma^+_{(v''=1)}$. Tilting of the laser narrow-band emission and positioning of more than 40 rovibronic lines of the NOε band has been allowed in agreement with the positioning of the lines from the NOβ band $B^2\Pi_{(v'=7)} \leftarrow X^2\Pi^+_{(v''=0)}$, recorded

simultaneously in a static cell filled with 50 mbar of NO. Accuracy in wavelength positioning is only dependent from the step by step increment of the laser tilting, and estimated of about 2.2 10^{-4} nm.

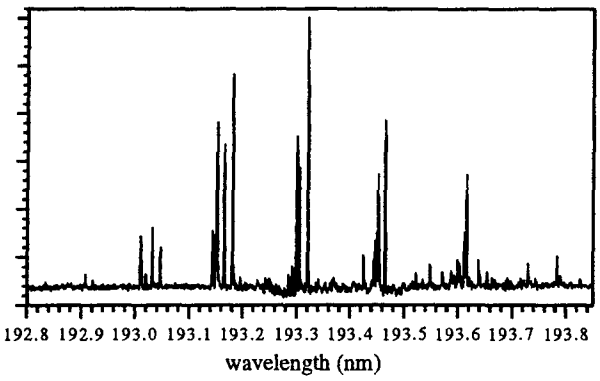

Fig(7):NOε band $D^2\Sigma^+_{(v'=0)} \leftarrow X^2\Sigma^+_{(v''=1)}$

Measurements are completed in a heated home made static (up to 1200 K) to record intensity lines evolutions versus temperature, and to chose the more sensitive transitions. The comparison with synthetic spectrum allows to complete the analysis for higher temperatures.

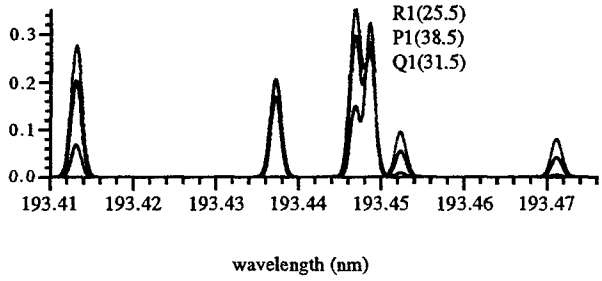

Fig(8): Temperaure measurement

From experiments and computed synthetic spectrum at numerous temperature, we can conclude that:

The $P_1(38.5)$, $R_1(25.5)$, and $Q_1(31.5)$ group of rotational lines of the NOε band, respectively at 51692.50, 51693.25 and 51693.75 cm^{-1}, is well identified to satisfy the requirements for the simultaneous measurement of density, temperature and velocity.

- Lines are closed to each other to minimized time of tilting of the excitation radiation to describe the entire profile of the group of lines.

- Lines are close to a reference line of the reference β-NO spectrum ($R_2(30.5)$ at 51693.25 cm^{-1}), which one will be used first to scale the tilting of the excitation before the recording of the lines profile, and second as the reference unshifted line for both laser excitation beam pathway used for Doppler Shift measurement.

- The intensity ratio of these transitions is sufficiently sensitive with the temperature in the temperature range of interest.

- The integrated intensity of the group of lines will be used for the absolute number density measurement after calibration with Rayleigh light scattering.

8.3 Interference with NOε band $D^2\Sigma^+_{(v'=0)} \leftarrow X^2\Sigma^+_{(v''=1)}$.

First, it has been observed that signal from plasma emission is in some order of magnitude weaker than fluorescence induced by the excimer laser, and thus can be neglected.

Secondary, the air flow of the TT1 wind tunnel has been probed with a broad-band laser excitation and detection has been tuned through a narrow-band filter (0.4

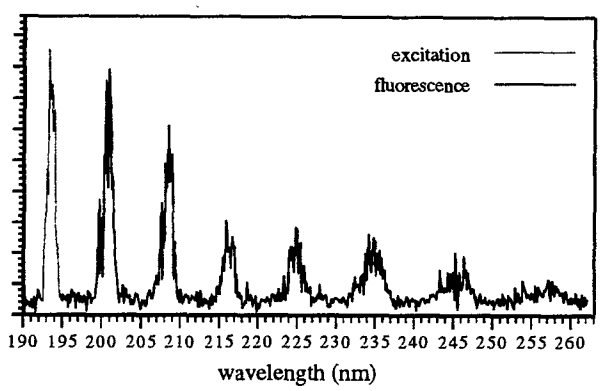

Fig(9): NO vibrational fluorescence de-excitation

nm FWHM) over a large spectral range in order to detect all the fluorescence of species present in the medium and excited with the ArF source. As a result of the broad-band excitation, only the NOε $\left(D^2\Sigma \rightarrow X^2\Sigma\right)$ fluorescence has been observed, from the resonant fluorescence centered on the excitation wavelength at 193.3 nm (Δv=0) up to 256.0 nm (Δv=7).

Because of all the potential interfering optical signals, it is important to verify that signals acquired are those from the NO fluorescence. We have to take into account

the possible reflection of the laser beam in the test chamber and close to the model, when measurements are performed in the shock layer at the vicinity of its surface. So, The fluorescence emission will be collected through the monochromator either from the (0-2) vibrational band (198 to 202 nm), or from the (0-3) vibrational band (206 to 210 nm). Less intense than the (0-1) but sufficiently far away from the Rayleigh peak, these fluorescence pathways are selected in order to maximize the fluorescence signal, minimize emission from the plasma flow and because its allows rejection of the elastically scattered laser light and reflection from the test chamber and surface of the model.

8.4 Absolute calibration of NO

For absolute calibration, the Rayleigh scattering is recorded in the test chamber with air at STP. Experiment is carried out with the complete optical setup and detection device, but precautions are taken to avoid reflection in the test chamber as the monochromator is tuned on the excitation laser radiation. By this way, fluorescence records and Rayleigh scattering are provided under identical experimental conditions. Thus, the terms related to the transmitivity of optical setup ε_c, and the size and probed volume $V_c\Omega_c$ may be ruled out in the expression of the ratio of fluorescence with Rayleigh scattering.

The air number density at STP and the differential Rayleigh cross section at the excitation wavelength are $N_{air}^{STP} = 2.4110^{19}\ part.cm^{-3}$ and $\sigma_{\nu_0}^{rayleigh} = 4.94810^{-26}\ cm^2$, respectively.

9. FLOW PARAMETERS MEASUREMENT

9.1 Analyze in the free plasma flow

Experiments are performed on both sides of the free jet axis and reveal a sufficient homogeneous region to locate the wide SiO_2 model and assure subsequently a 2D aerodynamic description of the boundaries conditions.

The unchanged rotational lines distribution and the constant fluorescence intensity point out a flat NO number density and temperature profiles in the free air flow section, 50 mm on either side from the jet axis.

The rotational temperature is estimated of about 1200 K and NO mole fraction of about $3.8\ 10^{-3}$.

The Doppler-shifted fluorescence signals provide a flat velocity radial distribution in the test section located at 190 mm from the nozzle exit. The constant value of 3325 $m.s^{-1}$ is corresponding to a supersonic flow with a Mach number close to Mach=4.9.

These results are in good agreement with the calculated parameters: v=3300 $m.s^{-1}$ and Mach=4.75, computed with the stagnation chamber conditions, the nozzle shape and assumption of a perfect gas flow in equilibrium upstream of the critical convergent throat and followed by a frozen expansion downstream in the nozzle divergent region.

No real discrepancy is observed between the four selected run

	Test run number	#1	#2	#3	#4
Trot	Rotational temperature (K)	1150	1200	1200	1150
[NO]	NO concentration	$3.8\ 10^{-3}$	$4.1\ 10^{-3}$	$3.7\ 10^{-3}$	$3.8\ 10^{-3}$
v	Velocity (m/s)	3325	3325	3275	3300

Table 2: TT1 wind tunnel results

9.2 Analyze in the shock layer

The flat plat model simulating a misalignment of tile with a step 3 mm height is placed on the homogenous region previously analyzed. The aerodynamic behavior of the supersonic high-enthalpy air flow impinging on a TPS SiO_2 model is shown in Fig(*). One observes mainly the bow shock which originates from the rounded leading edge and propagates laterally away from the surface. On the leading edge of the step, another less intense shock originates and rises up downstream the step.

Infra-red thermography doesn't reveals modification of bow shock in front of the model, at the location of the transition zone between the water cooling rounded leading edge and the SiO_2 surface. The picture reveals an important temperature gradient on the SiO_2 surface, up to 1500 K in the first part of the model and at the top of the step. On the contrary, in the last millimeters before the step, the temperature decreases down to 1100 k, just in the dark region at the foot of the step where a re-circulation zone can be expected. No LIF measurement has been done in front of the step because of the height reflection level of the laser beam on the step leading edge.

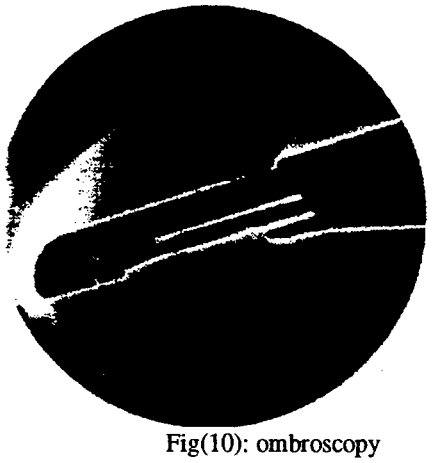

Fig(10): ombroscopy

Three sections located at 56, 112 and 156 mm from the rounded leading edge are investigated. The section S_{56} is 44 mm upstream the step, the S_{112} and S_{156} sections are downstream the step. On the two first sections reported on this picture, the two marks point out the place where a rise up of fluorescence has been observed by LIF at the boundary of the shock layer.

At the separation region between the free jet and the shock layer (estimated at $35 \leq y \leq 38$ mm), the NO-fluorescence signal increases exponentially because of NO vibrational excitation, i.e. a higher vibrational temperature and thus a higher number density of the of NO(v=1). As the transition considered in the NOε excitation process via $D^2\Sigma^+_{(v'=0)} \leftarrow X^2\Sigma^+_{(v''=1)}$ imply the v=1 vibrational level, increasing of the vibrational temperature is favorable to populate higher vibrational level, and thus increase the absorption process and the intensity of fluorescence detected at the crossing of the shock layer.

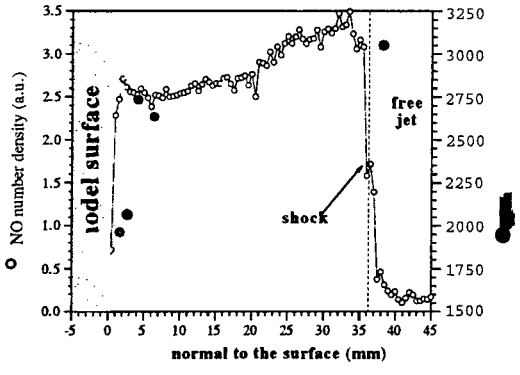

Fig(11): Profile of NO in the section S_{56}

The Fig(*) shows the fluorescence signal profile from the section S_{56}. Measurements are carried out with a spatial resolution of a 500 μm, from the free jet ($y > 0$) down to the surface ($y = 0$).

In the shock layer, intensity of fluorescence evolves weakly down to the surface of the model, and no rotational temperature gradient is observed. The number density thus do not vary significantly, indicating that NO number density is frozen into the shock layer.

In the two last millimeters ($0 \leq y \leq 2$ mm), the loss of signal is attributed to the cut of the spot size which is imputed to the intersection of the solid angle of the focused incident laser radiation with the surface of the model.

For $y \leq 5$ mm and down to the surface of the model, the weak rise up doesn't allow to conclude about a parietal recombination and indicate no signifiant creation of NO at the wall.

In the weakly dissociated flow, the current results do not confirm a predominant effect of wall recombination in comparison to the compression effect of the shock layer near the surface. The equilibrium conditions in the free jet upstream are 1200 K and 10^2 Pa, and the stagnation pressure behind the shock is evaluated to 1.9 10^3 Pa, namely 20-fold greater than the free jet static pressure. The same order of magnitude is observed on the fluorescence signal jump crossing the shock propagating laterally away from the model. If one considers first the fluorescence intensity with respect to the distribution of the NO $\left(X^2\Sigma^+_{(v''=1)}\right)$ in the absorbent rotational levels, and secondly, the very slight variation of the rotational temperature crossing the shock, then the NO concentration jump is in order of 22-fold greater in the shock layer than in the free jet. This value is assumed to be directly proportional to the difference of pressure crossing the shock layer.

The spatial resolution of 5 measurement points per millimeter allows to have an accurate description of the location and intensity of the shock. However, we have to consider than the real thickness of the shock is overestimated because of the vibrational excitation time lower than the rotational one.

The fluorescence emission results in the first section S_{56} are in good agreement with the ombroscopy picture which reveals only the shock location without giving information on the intensity ratio from both sides of the boundary shock layer.

The same results are obtained for the location of the second shock originating from the step, 15 mm behind the step (section S_{112}, see Fig(*)). Its lower intensity indicates

no real change in the vibrational relaxation and is confirmed by no significant evolution of the NO number density and rotational temperature.

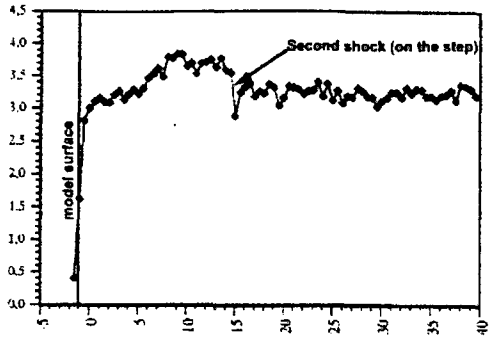

Fig(12): Profile of NO in the section S_{112}

The axial component of velocity is affected by the presence of the model. The profiles drawn from the three test sections of interest show a velocity gradient mainly located in the last millimeters close to the surface, in the region where a slight decrease of fluorescence has been previously observed.

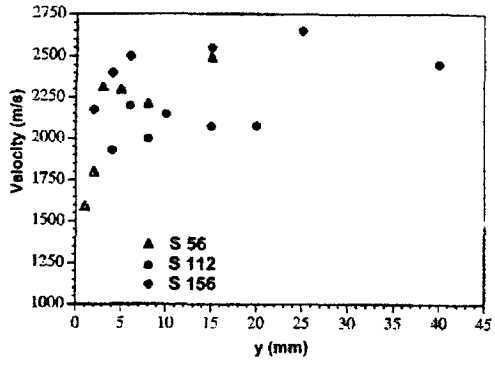

Fig(13): velocity in the shock layer

No discrepancy is observed for the axial component of the velocity across the shock front. Its value is estimated to 3300 ± 150 $m.s^{-1}$, which correspond to the initial free jet velocity. Upstream of the step, the thickness of the dynamic boundary layer is given at y = 5 mm in the first section. Under this limit, the velocity decreases continuously down to y = 1 mm to reach its lower value 1900 $m.s^{-1}$. The thickness of the dynamic boundary layer in front of the step can be expected to be of the same order of magnitude than the step height. One of the main feature of the velocity distribution in this section S_{112}, lies in the continuous increase in velocity, up to the limit of the shock generated at the top of the step. The lower value measured near the wall may be imputed to a deflection of the flow impinging on the step and a normal component of velocity non-negligible in comparison to the lower axial one. The most important gradient is observed 5 mm above the surface. For y > 5 mm, the axial value is approximately constant (2500$m.s^{-1}$) up to the limit of the secondary shock, then increases far off to reach its maximum value corresponding to the velocity of the free jet.

10. CONCLUSION.

The potential of LIF technique for instrumentation of continuous high enthalpy facilities has been demonstrated. NO number density, temperature and velocity has been measured in the supersonic air plasma free jet, as well as on a TPS model, allowing characterization of the aerodynamic behavior of the flow, especially at the misalignment of tiles.